

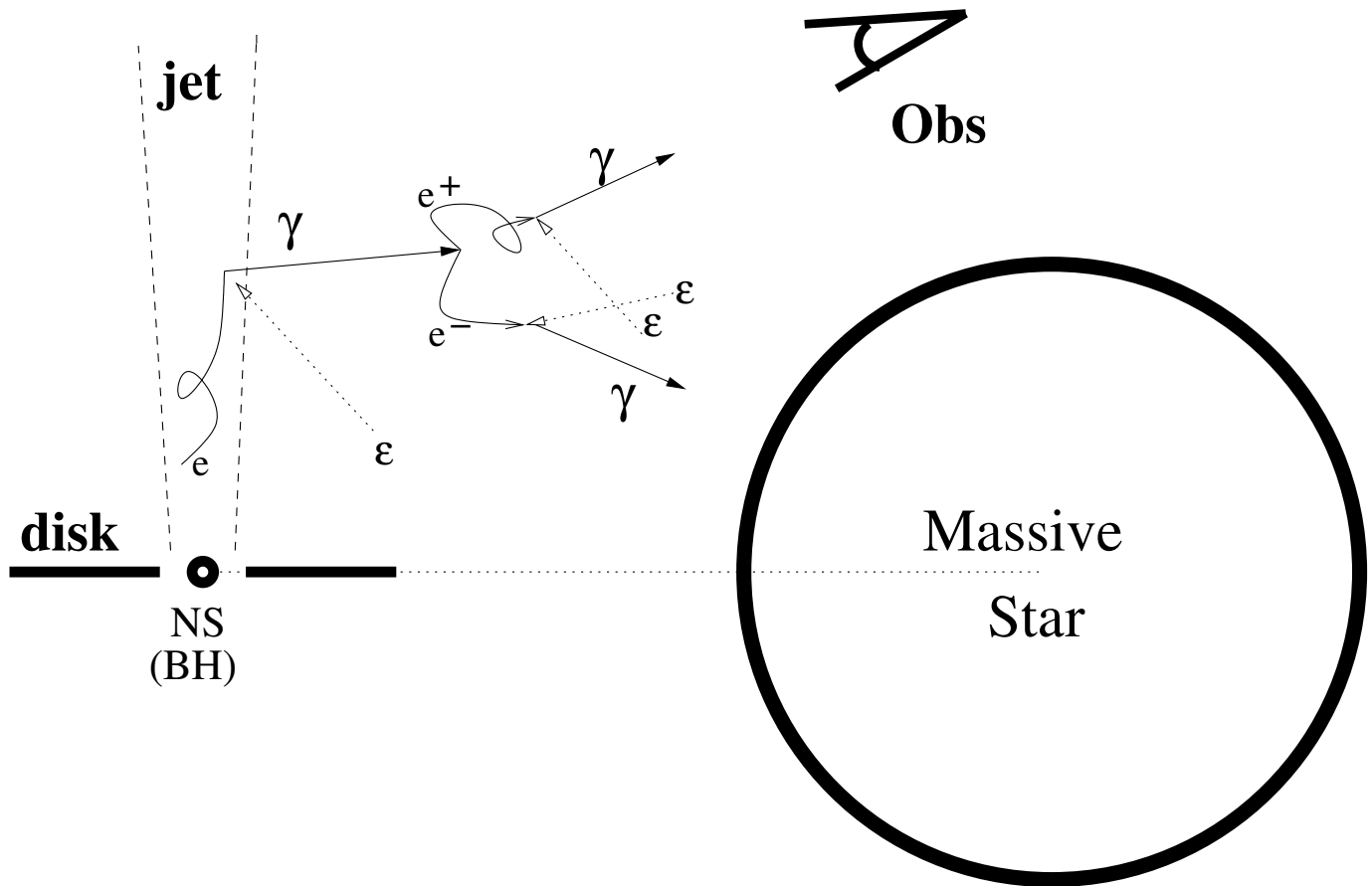
Gamma-rays from IC e^\pm pair cascades in massive binaries

Włoddek Bednarek

Department of Experimental Physics, University of Łódź, Poland

- IC e^\pm pair cascade model.
- Application to TeV γ -ray source **LSI 303+61^o**.
- Predictions for massive binary **Cyg X-1**.

Inverse Compton e^\pm pair cascade model



- Electrons injected into the jet with the power law spectrum.
- Comptonize stellar radiation: $e + \epsilon \rightarrow \gamma$.
- Gamma-rays absorbed: $\gamma + \epsilon \rightarrow e^\pm$.
- $e^\pm + \epsilon \rightarrow \gamma$ - cascade in the massive binary.

TeV γ -ray microquasars

- **LS I +61° 303:**

ellipticity: $e = 0.72$,

the semimajor axis: $5.3R_{\star}$,

inclination: $25^{\circ} < i < 60^{\circ}$,

azimuthal angle: $\omega = 70^{\circ}$.

radius of the star: $R_{\star} = 13.4R_{\odot}$,

surface temperature: $T_{\star} = 2.8 \times 10^4$ K.

- **LS 5039:**

ellipticity: $e = 0.35$,

the semimajor axis: $3.4R_{\star}$,

inclination: $25^{\circ} < i < 60^{\circ}$,

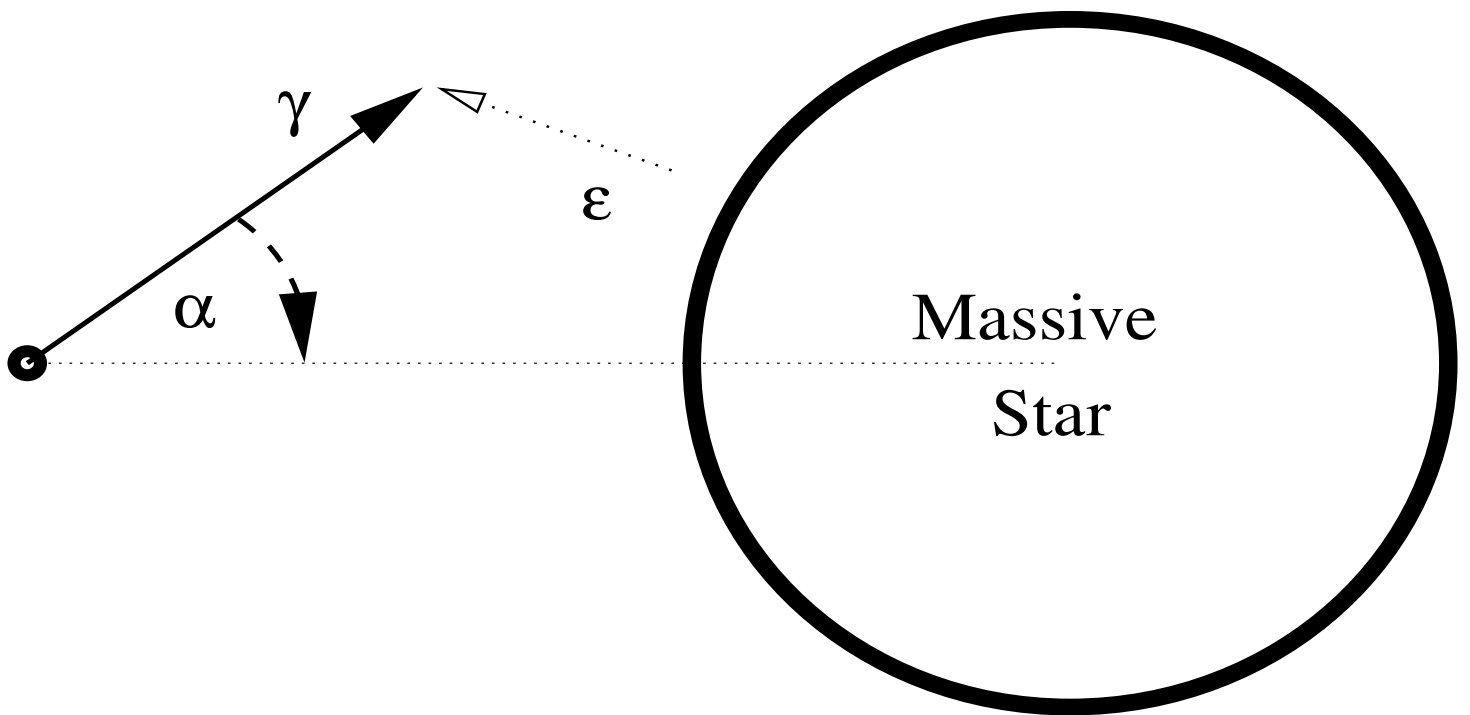
azimuthal angle: $\omega = 225^{\circ}$.

radius of the star: $R_{\star} = 9.3R_{\odot}$,

surface temperature: $T_{\star} = 3.9 \times 10^4$ K.

Absorption of TeV γ -rays


Obs



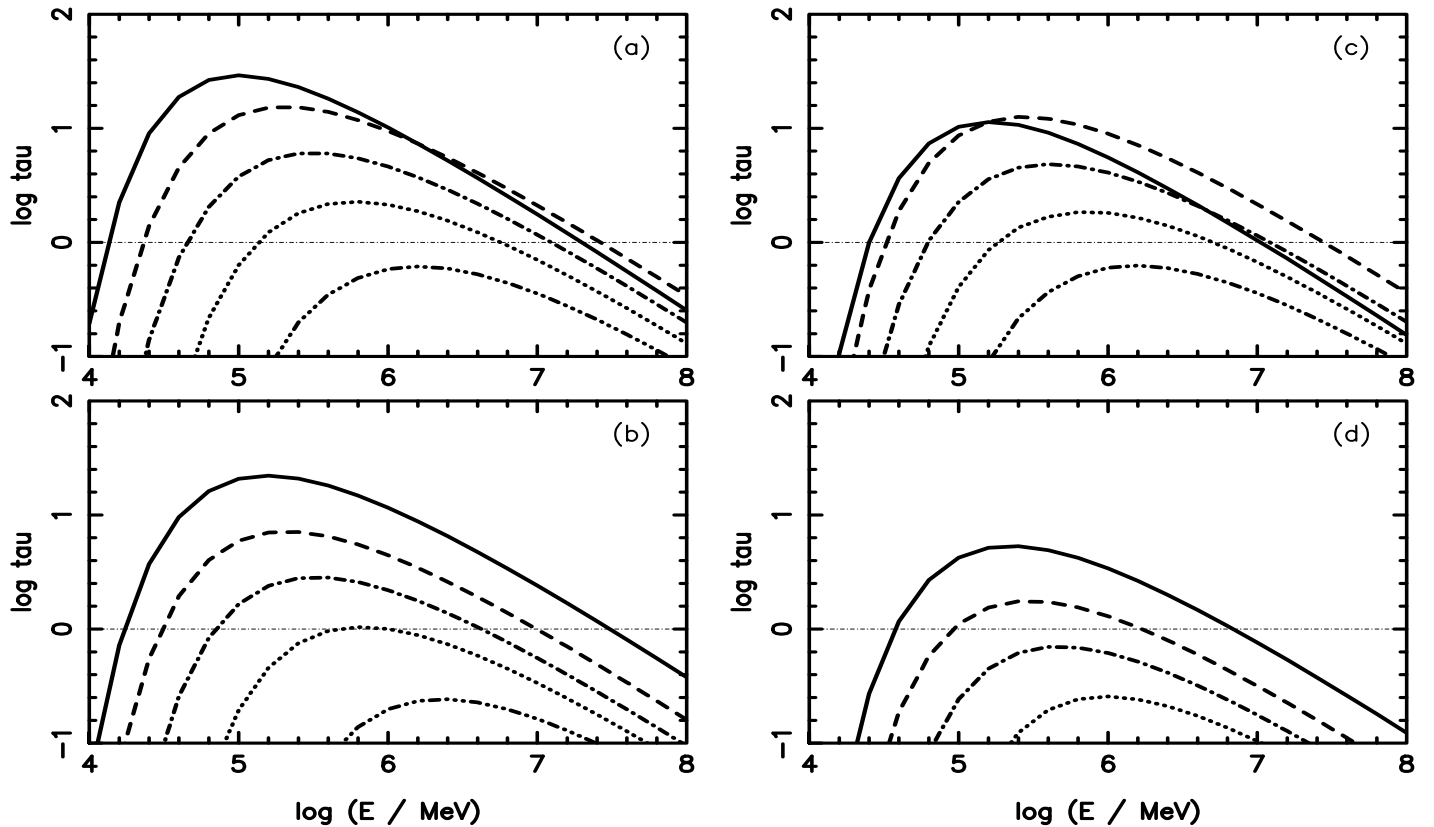


Figure 1: The optical depths for γ -rays (as a function of their energy) on e^\pm pair production in collisions with stellar photons. γ -rays are injected at two distances from the massive star in LS 5039 ($2.2r_\star$ (a) and $4.5r_\star$ (b)) and in LS I +61° 303 ($1.5r_\star$ (c) and $9.15r_\star$ (d)), corresponding to the periastron and the apoastron passages, respectively. Specific curves show the optical depths for the injection angles of γ -rays measured from the direction defined by the centers of the stars: $\alpha = 0^\circ$ (thick full curve, direction toward the massive star), 30° (thick dashed), 60° (thick dotted), 90° (thick dot-dashed), 120° (thin full), 150° (thin dashed), 180° (thin dotted) [Bednarek 2006a].

TeV γ -ray source LS I +61^o 303

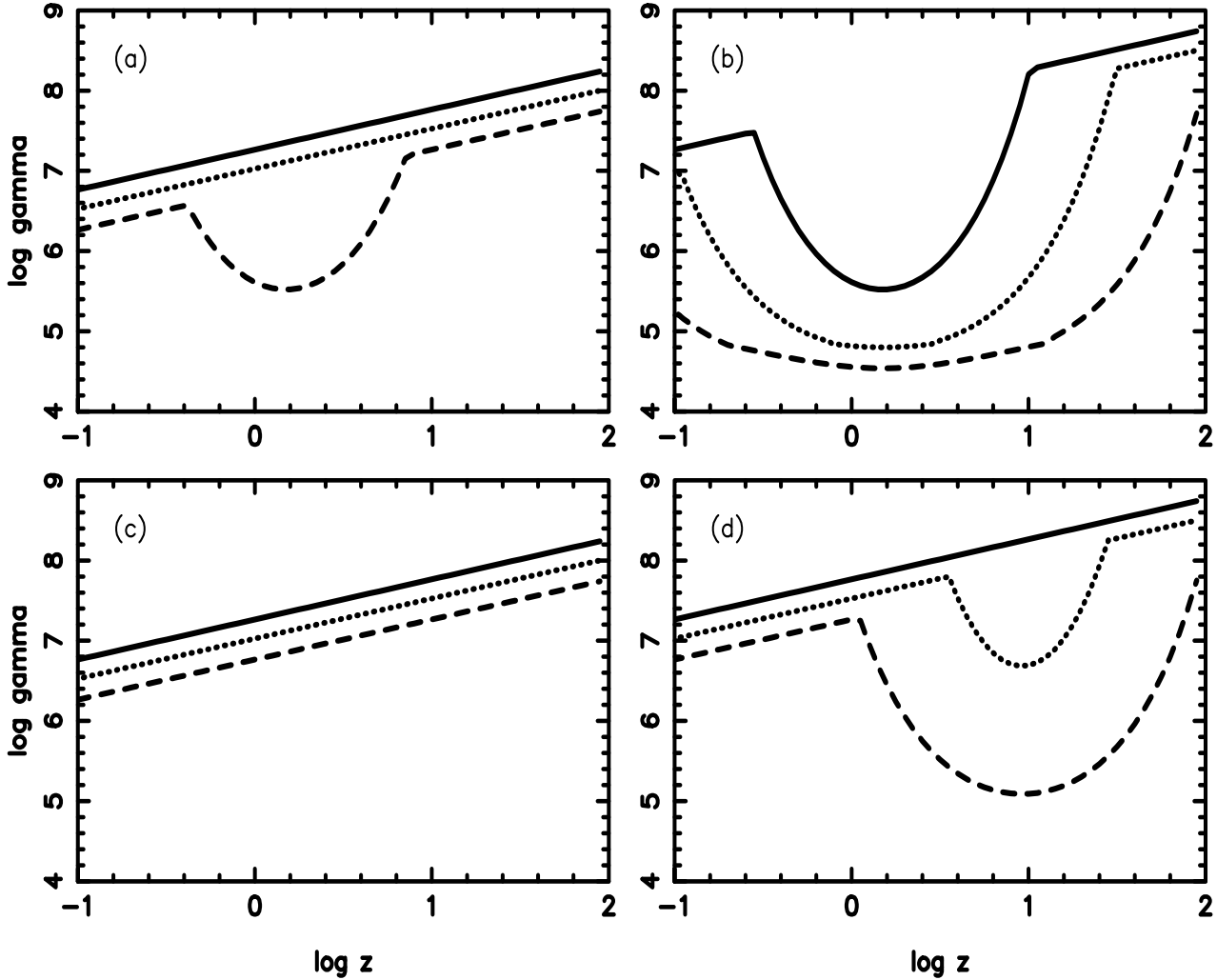


Figure 2: The maximum Lorentz factors of electrons as a function of the distance, z , from the base of the jet (measured in units of the stellar radius), for different acceleration efficiencies: $\xi = 0.3$ (full curves), $\xi = 0.1$ (dotted), and 0.03 (dashed). Specific figures show the results for two ratios of the magnetic field to accretion disk radiation energy densities counted at the base of the jet, equal to $\eta = 0.1$ (figures a and c), and 0.01 (b and d), for the periastron passage of the compact object (a and b) and for the apastron passage (b and d).

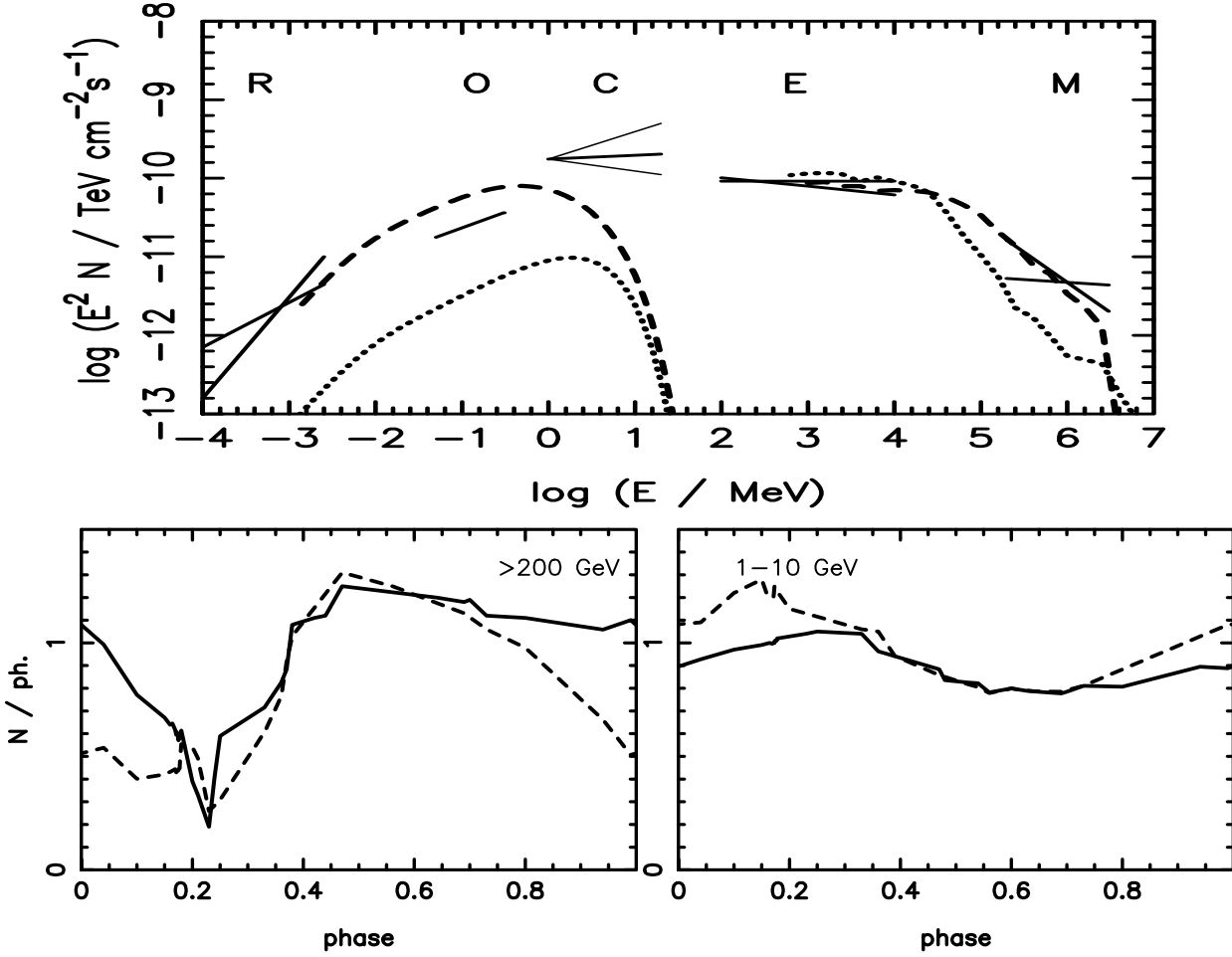


Figure 3: The multi-wavelength spectrum observed from LSI +61° 303 (X-ray data from the ROSAT (R - Goldoni & Mereghetti 1995) and the OSSE (O - Tavani et al. 1996), and in γ -rays from the COMPTEL (C - van Dijk et al. 1996), the EGRET (E - Kniffen et al. 1997), and the upper limits from the Whipple (W - $> 500 \text{ GeV}$ (Hall et al. 2003) and $> 350 \text{ GeV}$ (Fegan et al. 2005)) are compared with the inverse Compton and synchrotron spectra calculated in terms of IC e^\pm pair cascade model (for $\xi = 0.1$ and $\eta = 0.1$ and the electron spectrum $\propto E^{-2.4}$). The IC and synchrotron spectra are shown for the periastron passage (dotted curves), and for the phase 0.3 at which the maximum γ -ray flux is predicted (dashed). The γ -ray light curves in the energy range 1 – 10 GeV and $> 200 \text{ GeV}$ are shown in the middle figures for the inclination angles of the binary system $i = 30^\circ$ (full curve) and $i = 60^\circ$ (dashed) [Bednarek 2006b, in press].

Cyg X-1

Circular orbit; separation: $2.15R_{\star}$; inclination: $i = 33^{\circ} \pm 5^{\circ}$; radius of the star: $R_{\star} = 20R_{\odot}$; surface temperature: $T_{\star} = 3 \times 10^4$ K.

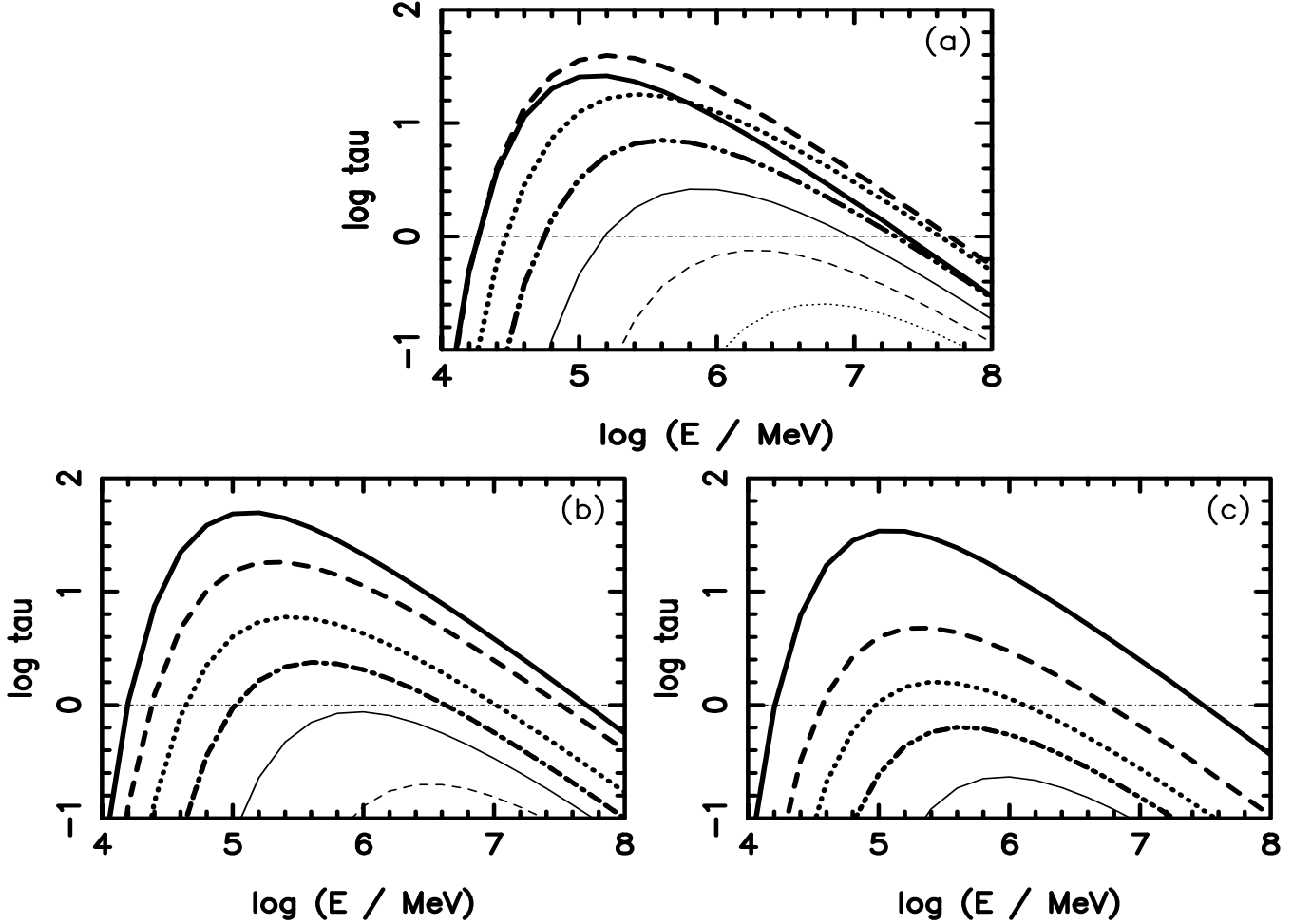


Figure 4: (a) The optical depths for γ -rays on e^{\pm} pair production in collision with stellar photons (as a function of their energy) injected at two distances from the massive star in Cyg X-1 and for selected angles measured from the direction defined by the centers of the stars, for $z = 1R_{\star}$ (a), $z = 5R_{\star}$, and $z = 20R_{\star}$ and the angle $\alpha = 0^{\circ}$ (thick full curve), 30° (thick dashed), 60° (thick dotted), 90° (thick dot-dashed), 120° (thin full), 150° (thin dashed), and 180° (thin dotted).

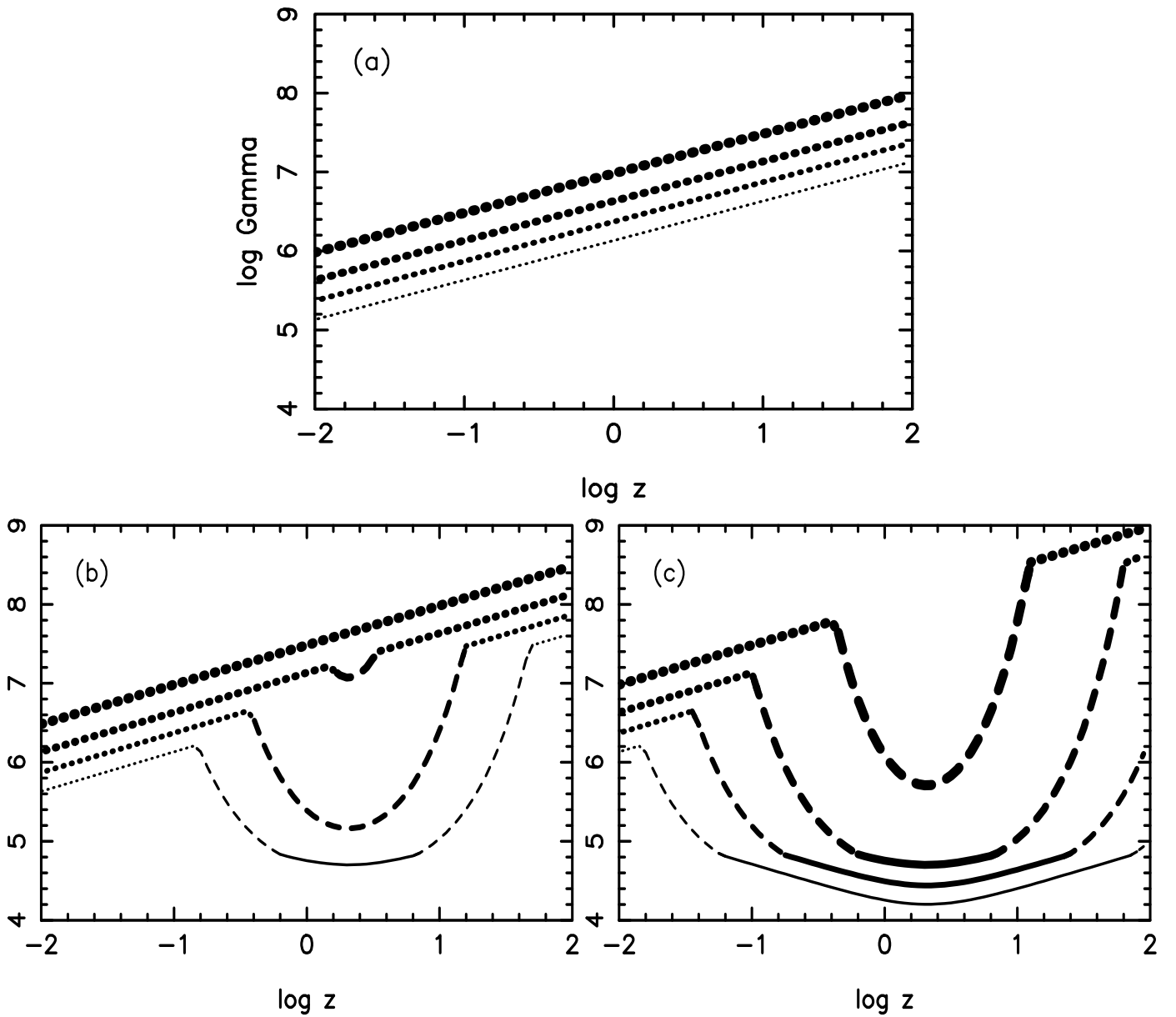


Figure 5: The maximum Lorentz factors of electrons as a function of the distance, z from the base of the jet (measured in units of the stellar radius) for different acceleration efficiencies: $\xi = 0.5$ (from the upper, thickest curve), 0.1, 0.03, and 0.01 (to the bottom, thinner curve) and two ratios of the magnetic field to disk radiation energy densities at the base of the jet equal to $\eta = 1$ (a), 0.1 (b), and 0.01 (c). The Maximum Lorentz factors are obtained from the comparison of the acceleration rate with the energy loss rate on synchrotron process (dotted lines), inverse Compton process in the Thomson regime (full curve) and the Klein-Nishina regime (dashed curves).

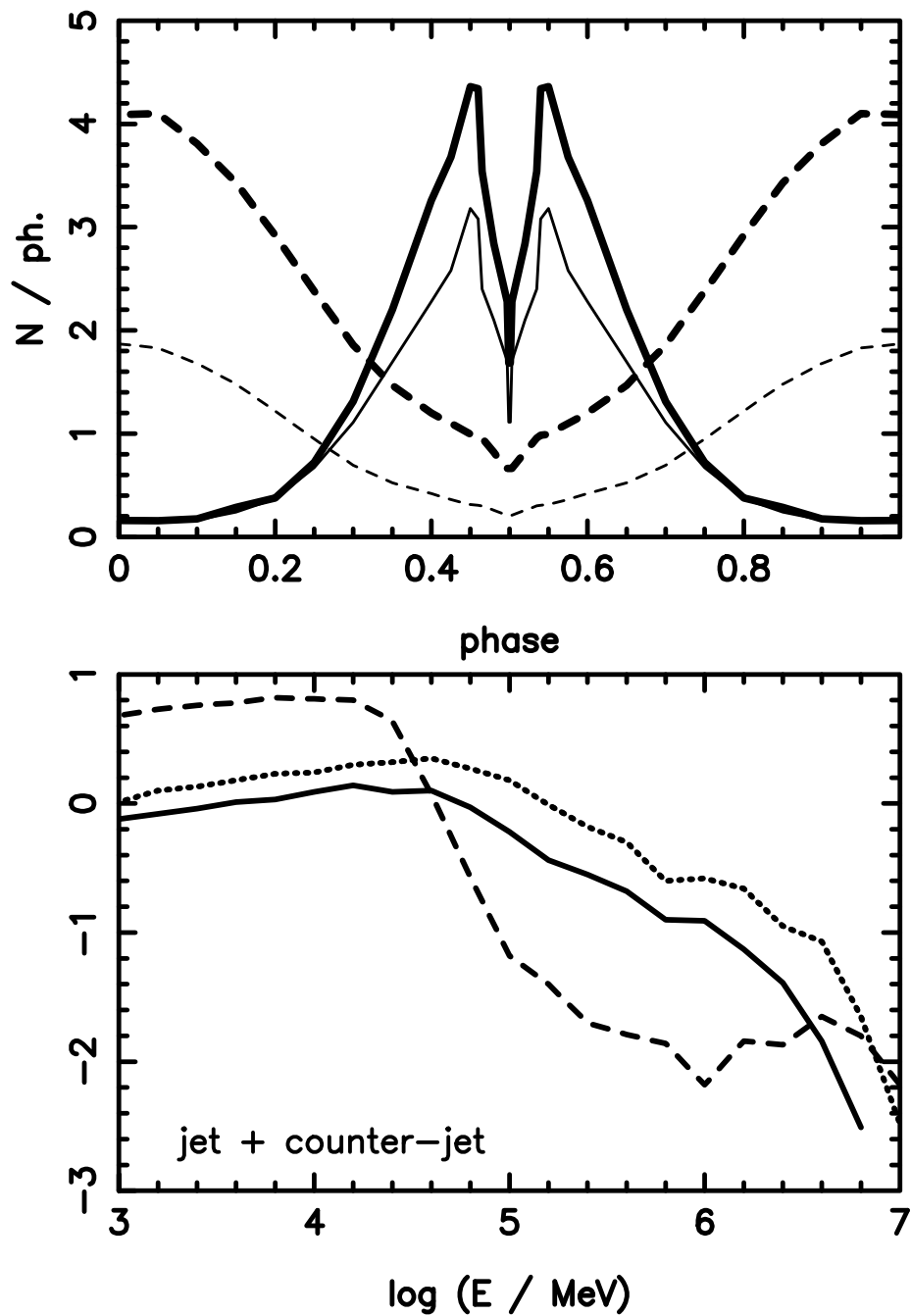


Figure 6: Gamma-ray light curves in the energy range 1-10 GeV (dashed curves) and >200 GeV (full curves) produced by electrons accelerated in the jets of Cyg X-1 for the acceleration parameters $\xi = 0.1$ and $\eta = 0.1$, γ -rays from electrons accelerated in the jet (thin curves) and in the jet + counter-jet (thick curves). The cascade IC γ -ray spectra produced by electrons in the jet and the counter-jet are shown for different phases of the compact object 0.0 (dashed curve), 0.45 (dotted), and 0.5 (full), measured from the location of the pulsar behind the massive star [Bednarek & Giovannelli 2006, submitted].

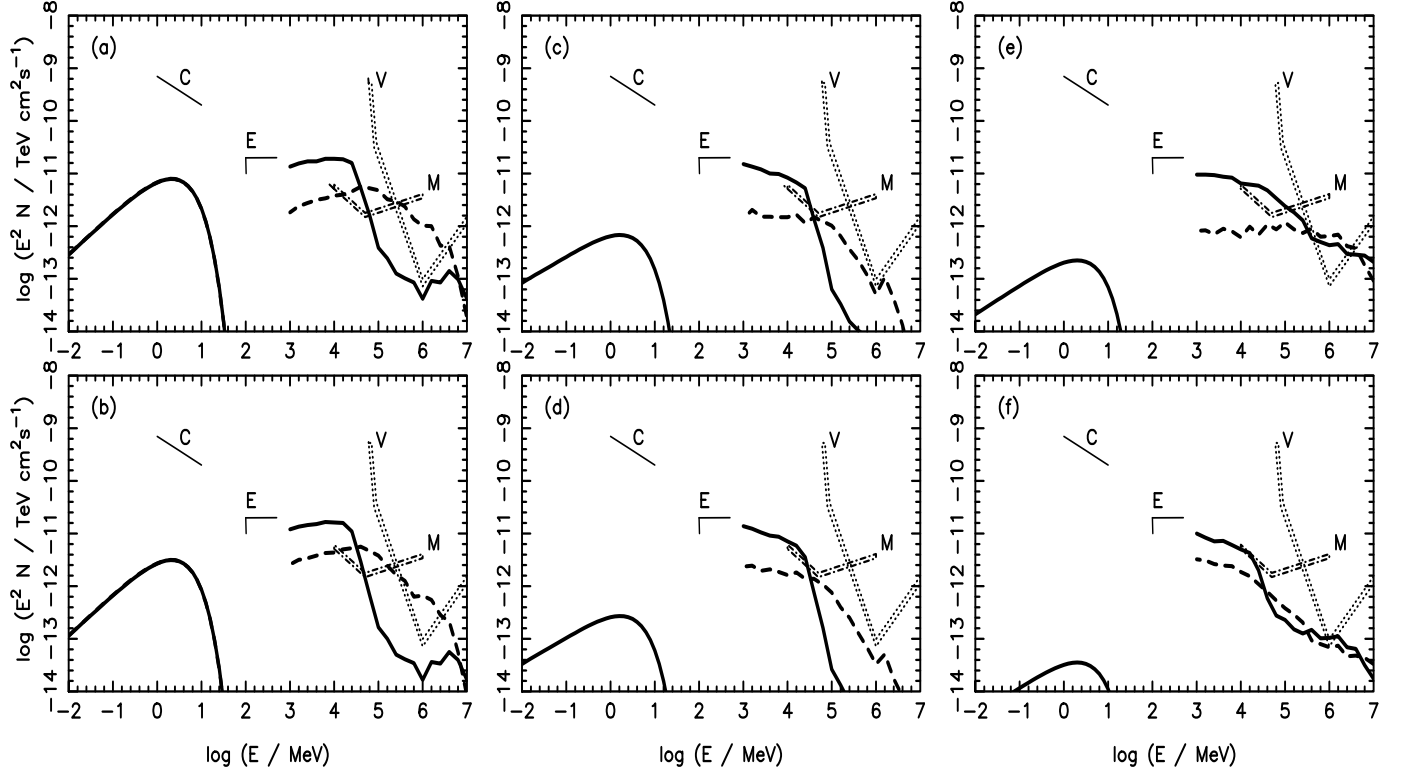


Figure 7: The multiwavelength spectrum of Cyg X-1, from different experiments, are compared with the γ -ray spectra calculated in terms of the cascade model for $\xi = 0.1$, $\eta = 0.1$ at the minimum TeV flux (at phase 0.2, full curve) and at the maximum flux (at the phase 0.45, dashed curve). The upper figures show the γ -ray spectra produced in the jet (after normalization to the EGRET upper limit), and the bottom figures from the jet + counter-jet. (a) and (b) are calculated for the differential spectral index of injected electrons equal to $\alpha = -2$ and the profile of energy transfer into the electrons according to $L(z) \propto z^{-2}$, (c) and (d) are for $\alpha = -2.6$ and $L(z) \propto z^{-2}$, and (e) and (f) for $\alpha = -2.6$ and $L(z) = \text{const}$. The synchrotron spectra produced by electrons in the jet are marked by the full curves.